

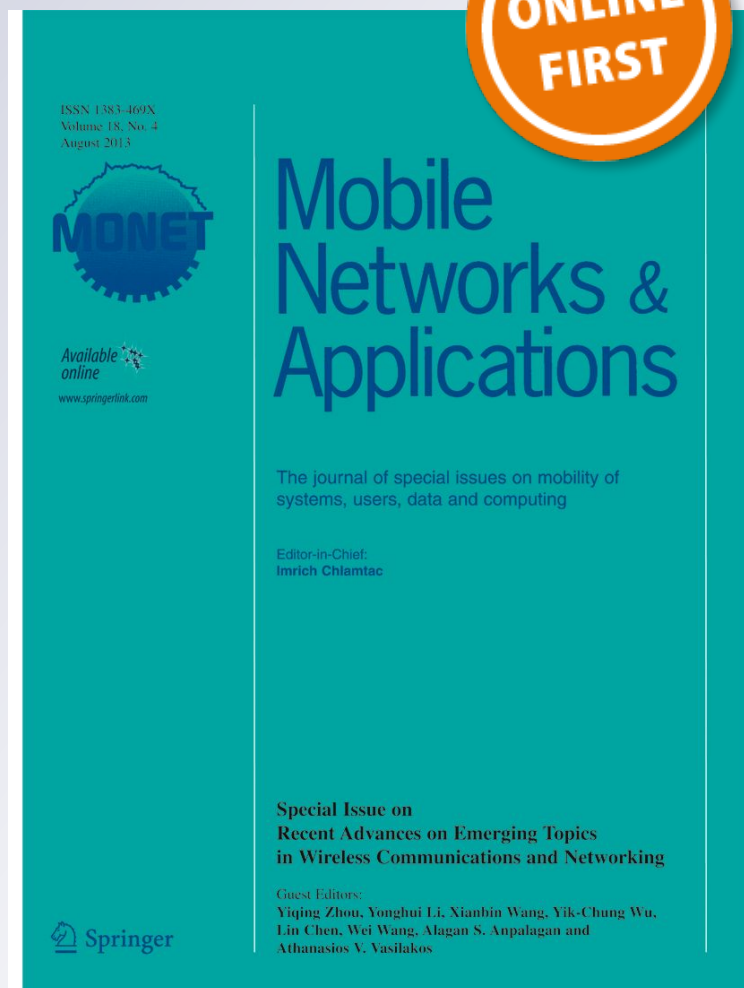
# *Performance Evaluation of Non-prefiltering vs. Time Reversal Prefiltering in Distributed and Uncoordinated IR-UWB Ad-Hoc Networks*

**Giuseppe Caso, Luca De Nardis, Mai T. Phuong Le, Flavio Maschietti, Jocelyn Fiorina & Maria-Gabriella Di Benedetto**

**Mobile Networks and Applications**  
The Journal of SPECIAL ISSUES on  
Mobility of Systems, Users, Data and  
Computing

ISSN 1383-469X

Mobile Netw Appl  
DOI 10.1007/s11036-017-0829-6



**Your article is protected by copyright and all rights are held exclusively by Springer Science +Business Media New York. This e-offprint is for personal use only and shall not be self-archived in electronic repositories. If you wish to self-archive your article, please use the accepted manuscript version for posting on your own website. You may further deposit the accepted manuscript version in any repository, provided it is only made publicly available 12 months after official publication or later and provided acknowledgement is given to the original source of publication and a link is inserted to the published article on Springer's website. The link must be accompanied by the following text: "The final publication is available at [link.springer.com](http://link.springer.com)".**

# Performance Evaluation of Non-prefiltering vs. Time Reversal Prefiltering in Distributed and Uncoordinated IR-UWB Ad-Hoc Networks

Giuseppe Caso<sup>1</sup> · Luca De Nardis<sup>1</sup> · Mai T. Phuong Le<sup>1</sup> · Flavio Maschietti<sup>2</sup> · Jocelyn Fiorina<sup>3</sup> · Maria-Gabriella Di Benedetto<sup>1</sup>

© Springer Science+Business Media New York 2017

**Abstract** Time Reversal (TR) is a prefiltering scheme mostly analyzed in the context of centralized and synchronous IR-UWB networks, in order to leverage the trade-off between communication performance and device complexity, in particular in presence of multiuser interference. Several strong assumptions have been typically adopted in the analysis of TR, such as the absence of Inter-Symbol / Inter-Frame Interference (ISI/IFI) and multipath dispersion due to complex signal propagation. This work has the main goal of comparing the performance of TR-based systems with traditional non-prefiltered schemes, in the novel context of a distributed

and uncoordinated IR-UWB network, under more realistic assumptions including the presence of ISI/IFI and multipath dispersion. Results show that, lack of power control and imperfect channel knowledge affect the performance of both non-prefiltered and TR systems; in these conditions, TR prefiltering still guarantees a performance improvement in sparse/low-loaded and overloaded network scenarios, while the opposite is true for less extreme scenarios, calling for the development of an adaptive scheme that enables/disables TR prefiltering depending on network conditions.

**Keywords** IR-UWB · Time hopping · Time reversal · Ad-hoc distributed networks · Multiuser interference · Inter-symbol interference

✉ Giuseppe Caso  
caso@diet.uniroma1.it

Luca De Nardis  
luca.denardis@uniroma1.it

Mai T. Phuong Le  
mai.le.it@ieee.org

Flavio Maschietti  
flavio.maschietti@eurecom.fr

Jocelyn Fiorina  
jocelyn.fiorina@centralesupelec.fr

Maria-Gabriella Di Benedetto  
mariagabriella.dibenedetto@uniroma1.it

<sup>1</sup> Department of Information Engineering, Electronics and Telecommunications (DIET), Sapienza University of Rome, Rome, Italy

<sup>2</sup> Department of Mobile Communications, EURECOM, Biot, France

<sup>3</sup> Department of Telecommunications, CentraleSupélec, Gif Sur Yvette, France

## 1 Introduction

Time Reversal (TR) is a prefiltering technique adopting a time reversed channel impulse response, and it has been proposed in the context of UWB communications in order to leverage the trade-off between communications performance and device complexity [1]. Previous work on the TR technique mostly focused on centralized and synchronous networks, as analyzed in [2], where TR synchronous transmissions with Power Control (PC) were compared to conventional non-prefiltered ones. In [3], the impact of TR on multiuser interference (MUI) in centralized networks was analyzed, showing that TR makes MUI distribution more *peaked*, thus leading to a communication performance increase. The impact of channel estimation errors on TR-prefiltered systems was discussed in [4], in which a mitigation scheme based on MMSE equalizer was also proposed, while in [5], a discrete-time model was presented

to investigate and compare robustness towards channel estimation errors of both non-prefiltered and TR-prefiltered schemes in a centralized and synchronous network. In [6], the advantages brought by TR in DoA-based positioning were also highlighted. While several studies have analyzed non-prefiltered UWB system performance under realistic scenarios, such as [7–11] on MUI, and [12] on Inter-Symbol / Inter-Frame Interference (ISI/IFI) in a Time Hopping (TH) scheme, strong assumptions have been typically adopted in the analysis of TR-based systems, such as the absence of ISI/IFI and multipath dispersion caused by complex propagation scenarios, in order to enable the derivation of theoretical performance bounds. Only recently, the impact of ISI/IFI on TR transmission was analyzed in [13], and a predistorted TR matrix was proposed for its suppression.

The above studies form the basis for the present work, that has the main goal of evaluating and comparing the performance of non-prefiltered vs. TR-prefiltered ad-hoc distributed UWB networks, where pairs of transmitters/receivers (TxS/RxS) communicate independently of each other, without synchronization and without PC. This scenario, almost unexplored in previous work on TR, turns to be relevant for the deployment of a next-generation communication and monitoring UWB sensor network [14]. UWB technology, integrated with the TR-prefiltering, is in fact a promising solution for the implementation of low-complexity and energy-efficient communication infrastructures, as explicitly required by the incoming 5G networking paradigm, in particular in the context of the mm-Wave communications and Internet of Things (IoT), as discussed in [15, 16] and [17].

The paper is organized as follows: Section 2 introduces the system model. A continuous-time model is first introduced and then modified into a discrete-time model, for a single Tx/Rx pair and an ad-hoc network. Within this framework, TR forms a special case of generic prefiltering scheme. Section 3 reports framework details and settings used to define different scenarios in which non-prefiltered and TR-prefiltered schemes have been analyzed. Simulation results are reported and discussed in Section 4, for both the single pair and the ad-hoc network. Finally, Section 5 concludes the work and introduces possible future research guidelines.

## 2 System model

In this Section, the system model is introduced. Continuous and discrete models for a single Tx/Rx pair are first shown, for both non-prefiltered and prefiltered schemes, focusing on Time Reversal in the latter case; models are then extended to a distributed and uncoordinated ad-hoc network, where multiple Tx/Rx pairs operate simultaneously.

### 2.1 Single Tx/Rx pair

A TH IR-UWB scheme, where the transmission time is divided into frames and frames are divided into chip times, is considered throughout the paper.

**Non-prefiltered scheme** In case of non-prefiltering, the signal transmitted in the  $n$ -th frame can be expressed as follows:

$$x(t) = b_n \sum_{m=0}^{N-1} s[m]p(t - mT_c), \tag{1}$$

where,  $T_c$  is the chip time and  $p(t)$  is the waveform associated to the symbol  $b_n$ , transmitted within the  $m$ -th chip time of the  $n$ -th frame. In general,  $p(t)$  is a UWB pulse and occupies bandwidth  $[-\frac{W}{2}, \frac{W}{2}]$ , so that its spectrum is zero for  $|f| > \frac{W}{2}$ . Moreover, the chip time used for transmission is decided through the *spreading* sequence  $\mathbf{s} = (s[0], \dots, s[N - 1])^T$ , that is a TH code of length  $N$ , for which all  $s[m]$  are zero except one, so that  $\|\mathbf{s}\|^2 = 1$ . Assuming that  $x(t)$  propagates over a multipath channel with impulse response  $h(t)$ , the received signal can be then expressed as follows:

$$\begin{aligned} y(t) &= x(t) * h(t) + n(t) \\ &= b_n \sum_{m=0}^{N-1} s[m]p(t - mT_c) * h(t) + n(t). \end{aligned} \tag{2}$$

If chip time and pulse duration are equivalent, then  $T_c = \frac{1}{W}$ ; moreover, if the channel impulse response has a finite delay spread  $T_d$  including  $L$  different paths, Eq. 2 is rewritten as follows:

$$y(t) = b_n \sum_{m=0}^{N-1} s[m] \sum_{l=0}^{L-1} h[l]p(t - (l + m)/W) + n(t). \tag{3}$$

An equivalent discrete model is obtained when Eq. 3 is projected onto  $\{p(t - \frac{m}{W}) : m = 0, \dots, (N + L - 1)\}$ . In this case, the discrete received signal  $\mathbf{y}$ , with dimensions  $(N + L - 1) \times 1$ , is expressed as follows [18]:

$$\mathbf{y} = \mathbf{C} \mathbf{s} b_n + \mathbf{n}, \tag{4}$$

where  $\mathbf{C}$  is the channel convolution matrix with dimensions  $(N + L - 1) \times N$ , having assumed a causal and finite channel impulse response with  $L = \frac{T_d}{T_c}$ . Moreover,  $\mathbf{n}$ , having same dimensions of  $\mathbf{y}$ , includes both thermal noise and ISI/IFI interference, with the latter arising from signal replicas experienced at previous frames, due to channel multipath. For a system modeled by Eq. 4, the optimal Rx scheme is the conventional All-Rake receiver (**All-Rake**), that is a filter matched to all multipath signal replicas. In this case, the Rx must know the time distribution of each path composing the channel impulse response. Knowing the

spreading sequence  $s$  and the channel convolution matrix  $C$ , a valid statistic for  $b_n$  is then obtained as follows:

$$\begin{aligned} z^{\text{AR}} &= \frac{Cs^T}{\|Cs\|} y \\ &= \frac{Cs^T}{\|Cs\|} (Csb_n + n). \end{aligned} \quad (5)$$

In severe multipath environments, design of **All-Rake** becomes complex and cost-ineffective. For this reason, several Partial-Rake strategies (**P-Rake**) have been proposed in order to reduce the **All-Rake** complexity. The One-Rake receiver (**1-Rake**), with a filter matched on the best SNR signal replica, can be seen as an extreme version of **P-Rake**, leading to minimum complexity at the price of reduced performance [19, 20].

**Prefiltered scheme** In case of prefiltering, the signal transmitted in the  $n$ -th frame can be expressed as the convolution between  $x(t)$  and a generic prefiltering impulse response  $h_p(t)$ :

$$x_p(t) = x(t) * h_p(t). \quad (6)$$

It follows that the received signal is:

$$y_p(t) = x_p(t) * h(t) + n(t), \quad (7)$$

with a discrete version as follows:

$$y_p = CPsb_n + n, \quad (8)$$

where, assuming same length for  $h_p(t)$  and  $h(t)$ ,  $P$  defines the prefiltering convolution matrix with dimensions  $(N + 2L - 1) \times (N + L)$ . In this scenario, the commonly adopted Rx scheme, referred to as **Pref 1-Rake**, is a filter matched on the peak of the overall (prefiltering + channel) impulse response:

$$\begin{aligned} z^{\text{Pref1R}} &= e_j^T y_p \\ &= e_j^T CPsb_n + e_j^T n, \end{aligned} \quad (9)$$

where  $e_j^T$  denotes the canonical vector with a one at the  $j$ -th position, where the peak is. It is worth noting that a prefiltered **All-Rake** scheme, referred to as **Pref All-Rake**, might be also implemented, at the price of increased complexity and costs.

The above general description maps to the Time Reversal scheme by choosing  $h_p(t) = h^*(-t)$ , so that the convolution of the signal with the reversed channel impulse response is made at the Tx. The overall filtering impulse response is thus the channel impulse response autocorrelation, having a peak in the center. **TR 1-Rake** is then matched on that peak, enabling the design of a simpler Rx in severe multipath environments, without any performance loss with respect to **All-Rake** alone (without TR) [6].

## 2.2 Distributed and uncoordinated ad-hoc network

An ad-hoc network is considered, where  $K$  Tx/Rx pairs communicate in an uncoordinated manner and independently from each other. Assuming the  $\tau$ -th pair as reference, signal  $x_\tau(t)$  propagates over  $h_\tau(t)$ ; the  $\tau$ -th Rx estimates the symbols transmitted by its paired Tx by considering the signals by other transmitters as unknown MUI interference. In the considered model, the receiver is a single user detector, not equipped with joint multiuser detection capabilities. This scenario differs from more traditional centralized network scenarios, where all transmissions are directed to a reference receiver, under two main aspects:

- *Synchronization*: while perfect timing might be assumed within each Tx/Rx pair, synchronization between different transmissions might be difficult to achieve, given the lack of a network reference clock due to the absence of a common Rx acting as network coordinator.
- *Power Control (PC)*: within centralized networks, the PC technique is used to adapt the transmitted signals, in order to solve the *near-far* problem, so that they all arrive at the reference Rx with equal power. PC is usually hard or even impossible to implement in a distributed and uncoordinated network.

**Non-prefiltered scheme** In case of non-prefiltering, a direct extension of Eq. 4 to  $K$  pairs can be obtained, by extrapolating the MUI term from the overall signal received by the reference Rx  $\tau$ :

$$y_\tau = C_\tau s_\tau b_{\tau,n} + \sum_{k=1}^{K-1} C_{k \rightarrow \tau} s_k b_{k,n} + n \quad k \neq \tau, \quad (10)$$

where  $C_{k \rightarrow \tau}$  introduces the convolution matrix of the channel between the  $k$ -th interfering Tx and the reference Rx.

**All-Rake** gives then the following decision variable:

$$\begin{aligned} z_\tau^{\text{AR}} &= \frac{(C_\tau s_\tau)^T}{\|C_\tau s_\tau\|} y_\tau \\ &= \frac{(C_\tau s_\tau)^T}{\|C_\tau s_\tau\|} C_\tau s_\tau b_{\tau,n} + \frac{(C_\tau s_\tau)^T}{\|C_\tau s_\tau\|} \sum_{k=1}^{K-1} C_{k \rightarrow \tau} s_k b_{k,n} \\ &\quad + \frac{(C_\tau s_\tau)^T}{\|C_\tau s_\tau\|} n \\ &= \|C_\tau s_\tau\| b_{\tau,n} + I_{\rightarrow \tau} + \hat{n}_\tau \\ &= \|C_\tau s_\tau\| b_{\tau,n} + I_{\rightarrow \tau} + S_\tau + v_\tau \quad k \neq \tau, \end{aligned} \quad (11)$$

where  $I_{\rightarrow \tau}$  represents the overall MUI interference towards the reference Rx  $\tau$ , and  $\hat{n}_\tau = S_\tau + v_\tau$  is the overall noise,

due to ISI/IFI interference ( $S_t$  term) and filtered thermal noise ( $v_t \sim \mathcal{N}(0, \frac{N_0}{2})$  term). In this case as well, a **1-Rake** might be used in order to reduce the Rx complexity.

**Prefiltered scheme** In case of prefiltering, Eq. 10 turns into:

$$y_{p,t} = C_t P_t s_t b_{t,n} + \sum_{k=1}^{K-1} C_{k \rightarrow t} P_k s_k b_{k,n} + n \quad k \neq t, \tag{12}$$

and the **Pref 1-Rake** decision variable follows Eq. 9, once the canonical vector  $e_{(j)_t}^T$  for the reference pair is defined. It follows that, in case of Time Reversal, definitions of **TR 1-Rake** and **TR All-Rake** are in accordance to the single user case, with the main difference that the performance equivalence between **All-Rake** and **TR 1-Rake** does not hold in a multiple Tx/Rx pairs scenario.

Equation 12 allows to highlight a peculiarity of TR-prefiltering when applied to a distributed network.

Within a centralized network, prefiltering is optimized by all TxS towards the reference Rx. As discussed in [3], this leads to a peaked MUI, and in turn to an overall network communication improvement. On the other hand, in a distributed network, each Tx/Rx pair is using prefiltering in order to optimize its own communication link. From a MUI perspective, this means that a reference pair will not necessarily experience peaked MUI, leading to a possible communication performance decrease. This aspect is evident when observing the second term of Eq. 12, showing that, for the  $k$ -th interfering pair, prefiltering convolution matrix  $P_k$  is optimized for the channel convolution matrix  $C_k$  and not for the interfering channel convolution matrix  $C_{k \rightarrow t}$ .

### 3 Analytical and simulation settings

With reference to the system model described in Section 2, analysis of **1-Rake**, **All-Rake**, **TR 1-Rake** and **TR All-Rake** receivers performance has been carried out by simulation. This Section reports the analytical and simulation settings used to define different scenarios in which the RxS have been compared.

**Channel model** The IEEE 802.15.3a channel model has been adopted for the generation of channel impulse response for the Tx/Rx pairs. In particular, the Line of Sight (LoS) model has been used, referred to in the standard as CM1. For each channel realization, stationarity within the observation time has been assumed, and a delay spread  $T_d = 50$  ns has been set, which includes the most essential replicas

[21]. Most of applicative scenarios have been analyzed holding the assumption of *perfect* channel knowledge; when otherwise specified, imperfect channel knowledge has been introduced by adopting the following impulse response:

$$\hat{h}(t) = \sqrt{(1 - \tau^2)}h(t) + \tau\xi(t), \tag{13}$$

where, after having normalized the variance of the channel,  $\xi$  is white Gaussian noise with standard deviation  $0 < \tau < 1$ . When  $\tau = 0$ , the impulse response is perfectly estimated, while  $\tau = 1$  means that  $\hat{h}(t)$  is independent from the corresponding  $h(t)$ .

**Network load** Two important parameters characterize the analysis of the considered distributed network: a) the number of Tx/Rx pairs  $K$ , and b) the number of chips in a transmission frame  $N$ . From these parameters, the network load  $NL = \frac{K}{N}$  has been defined; NL correlates the number of chips with the number of pairs that are using them. It follows from the definition that different values of NL can be obtained by assuming 1) a low  $K$  over a high  $N$ , 2) similar  $K$  and  $N$ , and 3) a high  $K$  compared to  $N$ . These three cases will be referred in the following to as **Low NL**, **Medium NL** and **High NL Scenarios**.

**Other settings** Monte Carlo simulations were carried out in order to provide consistent results. For each iteration,  $N_f = 5000$  frames were considered, divided into  $N$  chips of duration  $T_c = 1$  ns, and TxS/RxS were uniformly distributed in the area of interest imposing an average distance  $\bar{d}$  between pairs; while perfect timing were assumed within each Tx/Rx pair, random time shifts not exceeding the frame duration were artificially introduced in order to simulate asynchronous transmissions between the reference and each interfering signal. Concerning thermal noise, its variance was set to  $\sigma_n^2 = 1$ , and different SNR values were obtained by varying the useful signals power.

## 4 Results and discussions

This Section introduces the performance indicators used to compare the Rx schemes within different scenarios (Section 4.1), and reports the obtained simulation results, first focusing on the single Tx/Rx pair and then moving on the distributed network (Section 4.2).

### 4.1 Performance indicators

Bit Error Rate (BER) and Mutual Information  $I(X; Y)$  have been considered as performance indicators. In particular, denoting with  $X$  and  $Y$  the random variables associated to

the transmitted and received signals, respectively, mutual information  $I(X; Y)$  is used to derive system spectral efficiency and capacity, and it is defined as follows:

$$\begin{aligned}
 I(X; Y) &= H(Y) - H(Y|X) \\
 &= H(Y) - H(Z + N),
 \end{aligned}
 \tag{14}$$

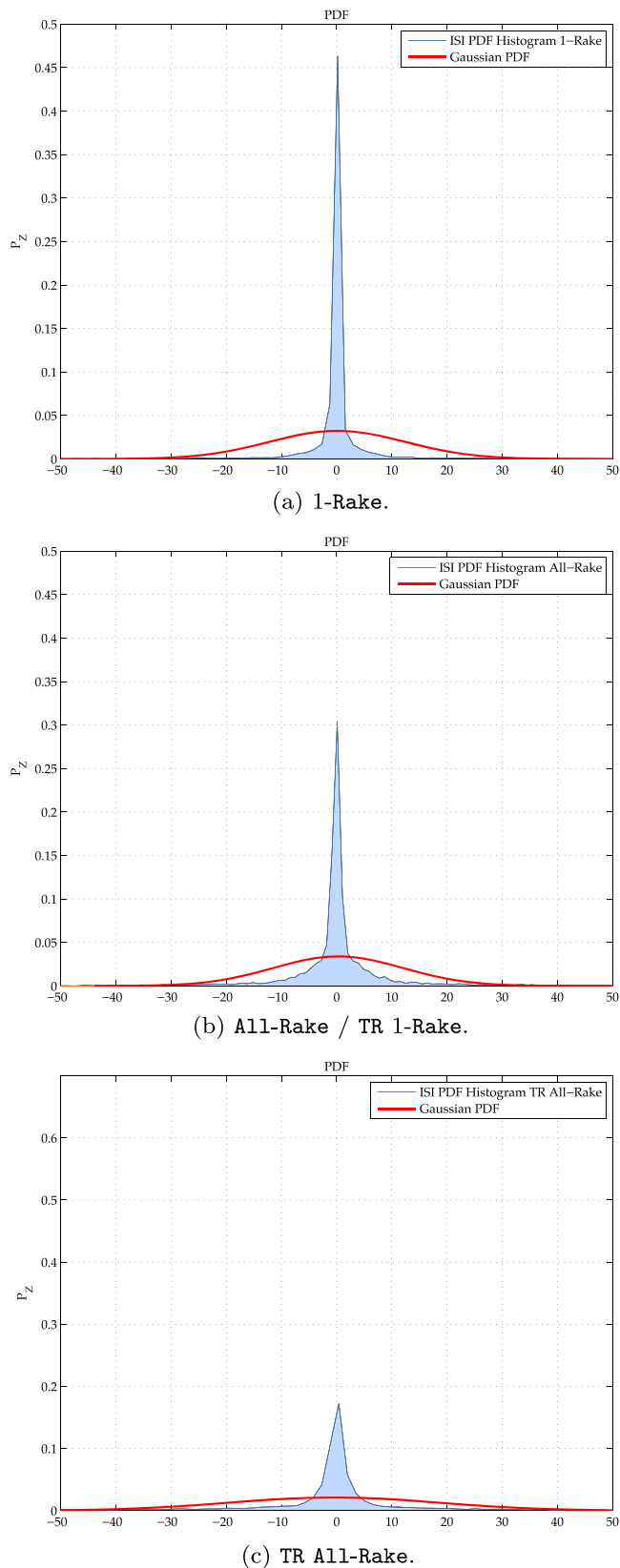
where  $H(\cdot)$  indicate differential entropies. Assuming that  $Y$  is composed by the random variables associated to a) the useful signal (referred to as  $X$ ), 2) the ISI/IFI/MUI (referred to as  $Z$ ) and 3) the thermal noise (referred to as  $N$ ), the second term of Eq. 14 is derived by considering  $Z$  and  $N$  independent over  $X$ . Furthermore, it is widely known that differential entropies are maximized when random variables have a Gaussian PDF [22]. In particular, assuming  $X \sim \mathcal{N}(0, \sigma_X^2)$ , entropy on the received signal is maximized; holding this hypothesis, in order to maximize the mutual information, that is maximize spectral efficiency and capacity, the interference random variable  $Z$  should be as less Gaussian as possible. A common Gaussianity indicator is the kurtosis value  $\kappa$ , that is equal to 3 for Gaussian distribution; the higher the kurtosis, the more peaked will be the PDF (the term *impulsive* will be also used in the following).

### 4.2 Results

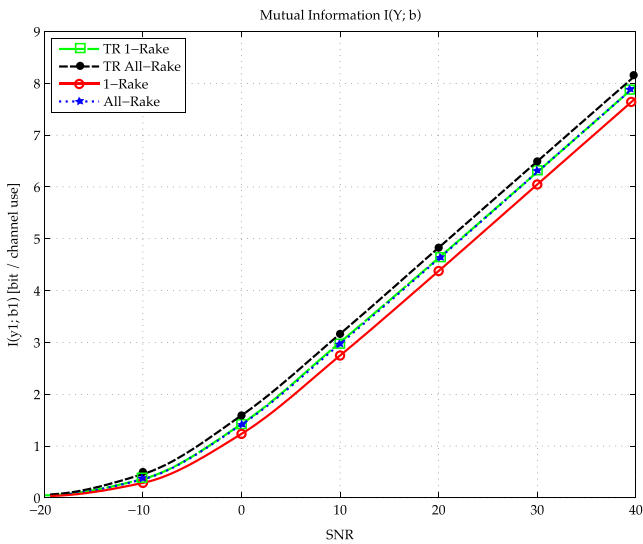
**Single Tx/Rx pair** When focusing on a single Tx/Rx pair, the impact of ISI/IFI and thermal noise on the Rx schemes have been analyzed. To do so, PDFs of ISI/IFI have been evaluated in the absence of thermal noise;  $I(X; Y)$  has been then derived in presence of thermal noise only, and in presence of both ISI/IFI and thermal noise.

Figure 1 reports the ISI/IFI PDFs in case of  $N = 10$  chips in a frame, for all Rx schemes (PDFs for **All-Rake** and **TR 1-Rake** are equivalent in the single pair scenario) and without thermal noise. Here and in the following analysis, Gaussian PDFs having same mean and variance are also reported for comparison. Results show that **1-Rake** achieves the most impulsive ISI/IFI PDF with respect to the other schemes; this is due to the fact that **1-Rake** can avoid most of ISI/IFI from previous frames given that it focuses on a single signal replica; from this perspective **TR All-Rake** is clearly the worst case, given that it considers all contributions coming from the overall channel autocorrelation. Moreover, the advantage of **1-Rake** is also related to the considered LoS scenario, where the LoS component is characterized by a significantly higher SNR compared to the other multipath components.

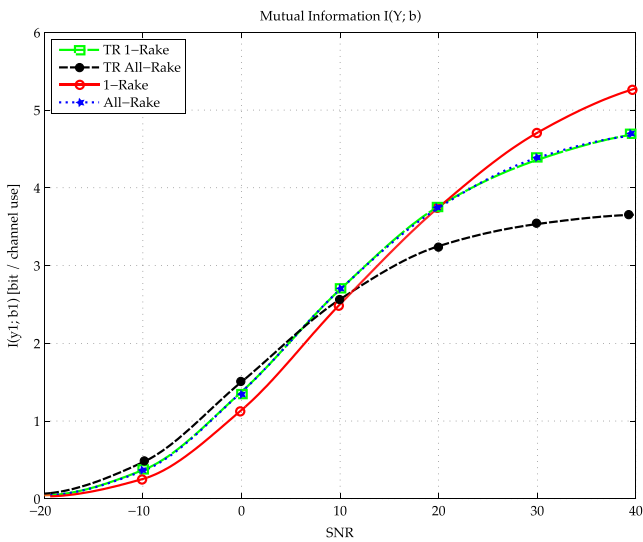
Figure 2 shows the mutual information for all Rxs as a function of SNR, in absence and presence of ISI/IFI



**Fig. 1** ISI/IFI PDFs in case of **1-Rake** (a), **All-Rake / TR 1-Rake** (b), and **TR All-Rake** (c) schemes ( $N = 10$ )



(a) Absence of ISI.



(b) Presence of ISI.

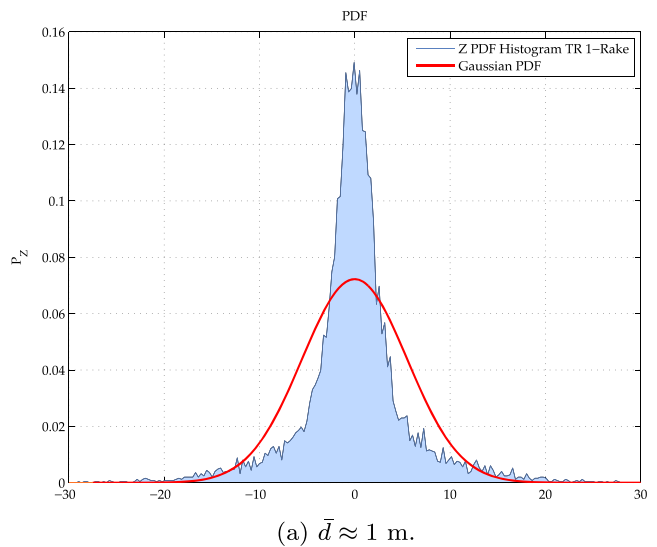
**Fig. 2**  $I(X; Y)$  for all Rx schemes, as a function of SNR and in case of absence of ISI (a) and presence of ISI (b) ( $N = 10$ )

(Fig. 2a and b, respectively). Results show that the presence of ISI generates a performance floor for all receivers, and in particular to the most ISI/IFI affected scheme, that is **TR All-Rake**. Paradoxically, the schemes that improve the performance when there is no ISI/IFI or when ISI/IFI is negligible in front of the Gaussian noise, are the ones that suffer the most from ISI/IFI when it becomes significant. It is because those schemes spread the signal in time and collect the energy of the signal on a more spread time. This highlights the importance of defining methodologies for ISI/IFI cancellation, such as the introduction of guard times between successive frames. It should be also noted however that the introduction of guard times may lead to significant

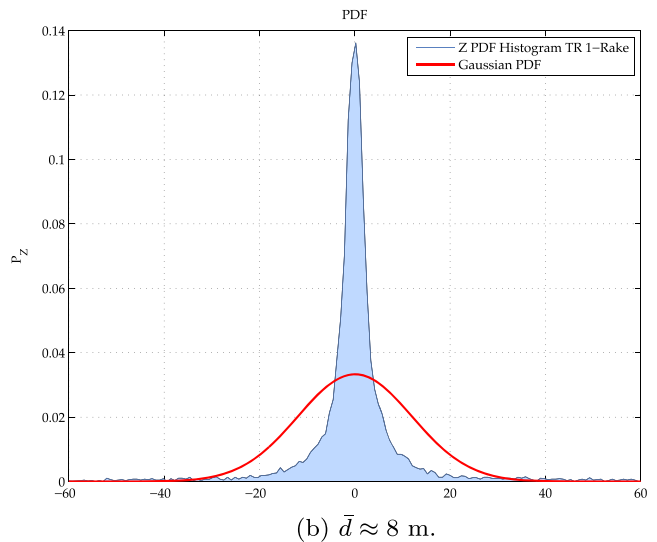
bitrate decrease, in particular in case of severe multipaths and Non LoS, where the channel delay spread might be high (in this work, as previously reported,  $T_d = 50$  ns has been fixed, that is a reasonable value in a LoS scenario).

**Distributed network** When focusing on the ad-hoc network, the impact of MUI and thermal noise have been analyzed. To do so, several network scenarios have been defined, as introduced in Section 3. For each scenario, PDFs of MUI have been evaluated in absence of ISI/IFI and high SNR, and mutual information has been then analyzed as a function of SNR. Impact of imperfect channel knowledge has also been analyzed in terms of BER.

Figure 3 shows the MUI PDFs for **TR 1-Rake** scheme, in case of Low NL Scenario (obtained by considering



(a)  $\bar{d} \approx 1$  m.



(b)  $\bar{d} \approx 8$  m.

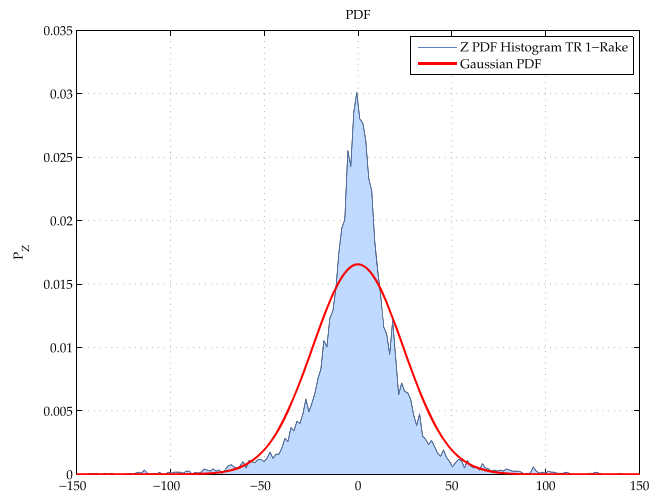
**Fig. 3** MUI PDFs for **TR 1-Rake** scheme in case of Low NL Scenario ( $NL = 0.25$ ,  $K = 2$  and  $N = 8$ ), and average distance between pairs  $\bar{d}$  of 1 m (a) and 8 m (b) (SNR = 20 dB)

NL = 0.25,  $K = 2$  and  $N = 8$ ) and an average distance  $\bar{d}$  between pairs of 1 m and 8 m (Fig. 3a and b), respectively. In order to compare the performance with the other Rx schemes, Table 1 reports the value of kurtosis for the Rx schemes in the same scenario (here and in the following, **1-Rake** kurtosis is omitted for sake of simplicity).

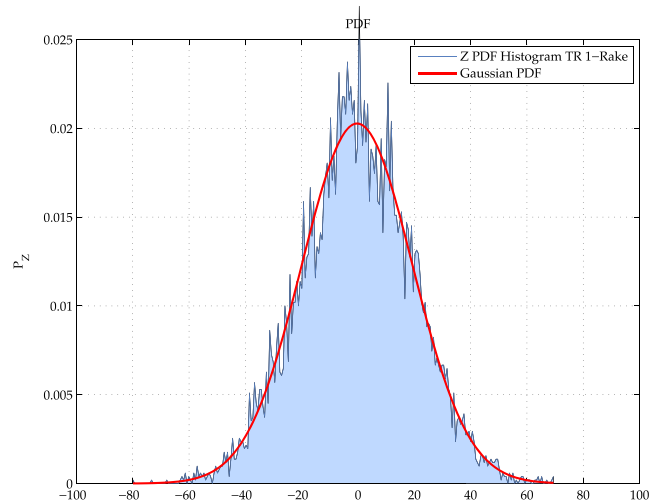
Results highlight several properties: first of all, due to the impulsive nature of TH-UWB signals, MUI is not Gaussian, irrespectively of the Rx scheme, and this is clear when considering kurtosis reported in Table 1. Moreover, MUI distribution strongly depends on the network area, underlining a direct relationship between performance and spatial density. This is due, in particular, to the lack of PC, that leads to more impulsive PDFs as the network area increases. From this perspective, on one hand, Time Reversal seems to be more sensitive to the network size, given that its kurtosis significantly varies while changing the area; on the other hand, it outperforms the non-prefiltered scheme in case of sparse (large areas) networks, suggesting its possible application to large and low loaded sensor networks.

Similarly to the Low NL Scenario, Fig. 4 shows the MUI PDFs for **TR 1-Rake** scheme, in case of Medium NL and High NL Scenarios (obtained by considering NL = 0.5,  $K = 10$  and  $N = 20$ , and NL = 4,  $K = 20$  and  $N = 5$ , respectively), and an average distance between pairs  $\bar{d} = 4$  m. Moreover, Table 2 reports the value of kurtosis for all Rx schemes and same scenarios. MUI PDFs shape and, in general, the decrease of kurtosis when compared to the previous case highlight that MUI distributions are approaching a Gaussian distribution, as the number of users increases in the network. Moreover, they show that **All-Rake** slightly outperforms the TR schemes in Medium NL, while the opposite happens in High NL Scenario. Results are confirmed by Fig. 5, showing the mutual information for the Rx schemes in the two scenarios, as a function of SNR.

Results suggest that, when applied to distributed and uncoordinated networks, TR schemes are more sensitive to the lack of PC and do not help in achieving impulsive MUI, given that, as observed in Section 2.2, the prefiltering matrix is optimized for each transmission link and not for the interference towards the receiver of the reference pair. However, this unwanted effect is mitigated in some scenarios, such as a) sparse and poorly loaded and b) highly



(a) Medium NL Scenario (NL = 0.5,  $K = 10$  and  $N = 20$ ).



(b) High NL Scenario (NL = 4,  $K = 20$  and  $N = 5$ ).

**Fig. 4** MUI PDFs for **TR 1-Rake** scheme in case of Medium NL (a) and High NL (b) Scenarios (SNR = 20 dB and  $\bar{d} \approx 4$  m)

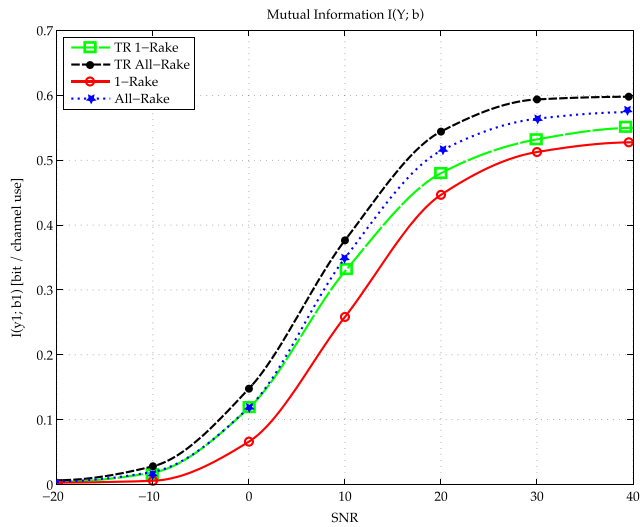
loaded networks, where **TR 1-Rake** outperforms traditional **All-Rake**. It is also observed that **TR All-Rake** outperforms all Rx schemes in both Medium NL and High NL Scenarios, but this is obtained at the price of higher Rx hardware complexity.

**Table 1** Kurtosis of MUI PDFs for all Rx schemes, in case of Low NL Scenario (SNR = 20 dB)

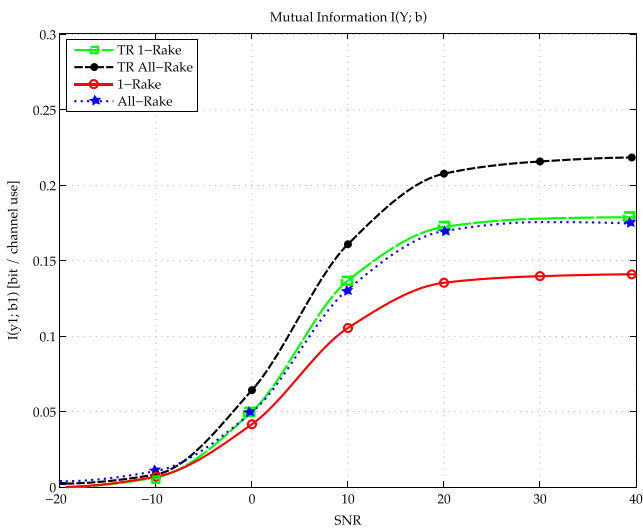
Receiver	Low NL ( $\bar{d} \approx 1$ m)	Low NL ( $\bar{d} \approx 8$ m)
All-Rake	8.9	9.8
TR 1-Rake	7.68	17.89
TR All-Rake	5.31	12.24

**Table 2** Kurtosis of MUI PDFs for all Rx schemes, in case of Medium NL and High NL Scenarios (SNR = 20 dB and  $\bar{d} \approx 4$  m)

Receiver	Medium NL	High NL
All-Rake	6.8	3.1
TR 1-Rake	6.44	3.22
TR All-Rake	5.94	3.18



(a) Medium NL Scenario (NL = 0.5, K = 10 and N = 20).

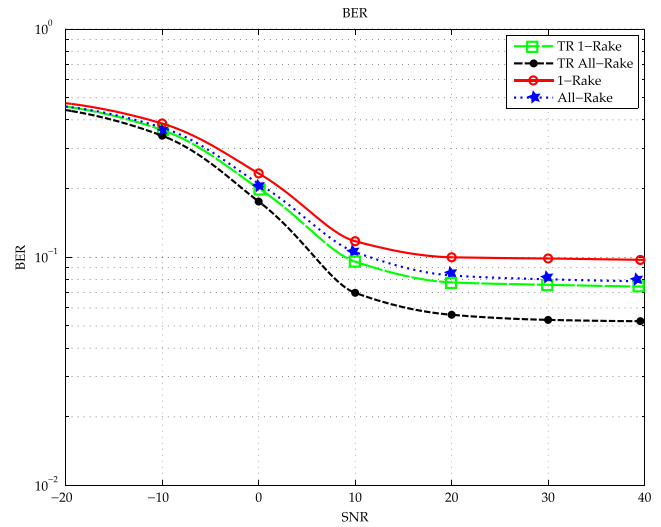


(b) High NL Scenario (NL = 4, K = 20 and N = 5).

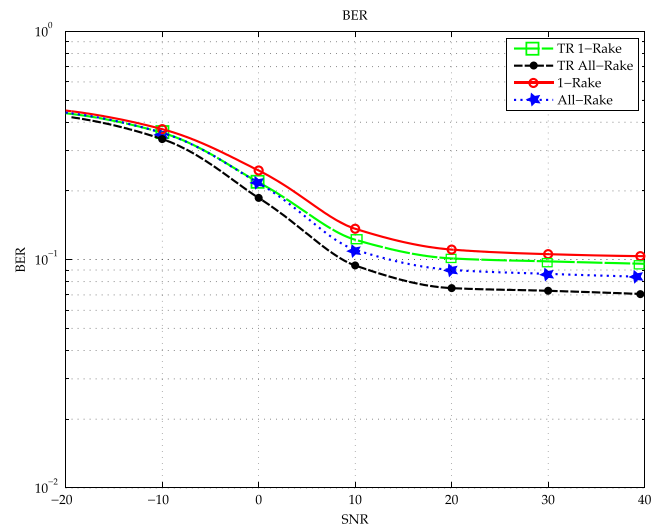
**Fig. 5**  $I(X; Y)$  for all Rx schemes, as a function of SNR in case of Medium NL (a) and High NL (b) Scenarios

Another performance comparison was carried out in the hypothesis of imperfect channel knowledge, modeled as described at the beginning of Section 3. In this case, analysis is provided in terms of BER, given that mutual information definition implies perfect channel knowledge. Figure 6 shows BER for all Rx schemes as a function of SNR, in case of Medium NL Scenario and perfect and imperfect channel knowledge ( $\tau = 0$  and  $\tau = 0.01$ , Fig. 6a and b, respectively).

Results show that, as expected, TR schemes are the most degraded ones in the case of imperfect channel knowledge. **TR 1-Rake** turns to be worse than **All-Rake**, while **TR All-Rake** significantly degrades its own performance.



(a) Perfect channel knowledge ( $\tau = 0$ ).



(b) Imperfect channel knowledge ( $\tau = 0.01$ ).

**Fig. 6** BER for all Rx schemes, as a function of SNR in case of Medium NL Scenario, perfect channel knowledge ( $\tau = 0$ ) (a) and imperfect channel knowledge ( $\tau = 0.01$ ) (b)

These results, highlighting the need of reliable and accurate channel estimation techniques when TR schemes are applied to the UWB technology, are furtherly confirmed by

**Table 3** Percentage increase of BER floor with imperfect channel knowledge ( $\tau = 0.1$ )

Receiver	BER Floor Increase
<b>1-Rake</b>	7%
<b>All-Rake</b>	15%
<b>TR 1-Rake</b>	58%
<b>TR All-Rake</b>	65%

observing Table 3, where the percentage increase of BER floor with  $\tau = 0.1$  is reported for all Rx schemes.

## 5 Conclusions and future work

A performance comparison between non-prefiltered and Time Reversal prefiltered UWB communications has been presented. Differently from other works, that focused on centralized and synchronized networks, the present analysis was carried out for ad-hoc distributed and uncoordinated networks, that model further applicative scenarios for the UWB technology, particularly relevant for next-generation communication and monitoring networks. More realistic assumptions, such as the presence of ISI/IFI due to propagation multipaths has been also taken into account.

Results showed that, in case of a single ISI/IFI affected Tx/Rx communication link, higher complex **TR All-Rake** scheme does not provide performance improvement, given that it increases signals length, thus worsening the ISI/IFI effect. Furthermore, performance equivalence of **TR 1-Rake** and **All-Rake** schemes is confirmed in presence of ISI/IFI.

When focusing on the ad-hoc network, it was first shown that, independently of the adopted Rx scheme, the MUI PDF, although not Gaussian, tends more to Gaussianity (its kurtosis tends to 3) as the number of users in the network increases. Moreover, given the lack of PC that mitigates the near-far problem, the MUI distribution also depends on the network spatial density, and this aspect is particularly relevant for TR schemes. However, when perfect channel knowledge is assumed, **TR 1-Rake** outperforms **All-Rake** in low loaded/sparse and highly loaded networks, while the opposite was observed in case of imperfect channel knowledge; this underlines the need for effective channel estimation and appropriate ISI/IFI mitigation, when Time Reversal is applied to ad-hoc UWB networks.

Future investigations will extend the model proposed in this work. In particular, on one hand, a more detailed theoretical analysis that considers Poisson Point Process for user positions modeling and other channel models, such as the IEEE 802.15.3a NLoS CMs, is currently being addressed, together with the development of ISI/IFI removal techniques through predistorted TR-based prefiltering matrices, thus extending the solution proposed in [13]. On the other hand, the design of adaptive Tx/Rx devices, that might adapt their communication by choosing between non-prefiltered and prefiltered schemes with respect to the network scenario (in terms of load, spatial distribution, device position and mobility) would form an appealing added feature, in particular in the application of TR prefiltering to cognitive radio scenarios.

## References

1. Strohmer T, Emami M, Hanses J, Papanicolaou G, Paulraj A (2004) Application of Time-Reversal with MMSE equalizer to UWB communications. In: IEEE Global Telecommunications Conference, vol 5. IEEE Press, pp 3123–3127
2. Popovski K, Wisocki BJ, Wisocki TA (2007) Modelling and comparative performance analysis of a Time-Reversed UWB system. Springer EURASIP J. Wirel Commun Netw 1:1–11
3. Fiorina J, Capodanno G, Di Benedetto M.-G. (2011) Impact of time reversal on Multi-User interference in IR-UWB. In: IEEE International Conference on Ultra-Wideband. IEEE Press, pp 415–419
4. Bizaki KH, Alizadeh S (2012) Mitigation of channel estimation error in TR-UWB system based on a novel MMSE equalizer. Springer Ann Telecommun 68(5):317–325
5. Ferrante GC (2015) Shaping interference towards optimality of modern wireless communication transceivers. PhD Thesis. La Sapienza, University of Rome and Supélec
6. De Nardis L, Fiorina J, Panaitopol D, Di Benedetto M-G (2013) Combining UWB with time reversal for improved communication and positioning. Springer Telecommun Syst 52(2):1145–1158
7. Giancola G, De Nardis L, Di Benedetto MG (2003) Multiuser interference in Power-Unbalanced ultra wide band systems: Analysis and verification. In: IEEE Conference on Ultra Wideband Systems and Technologies. IEEE Press, pp 325–329
8. Fiorina J, Domenicali D (2009) The non validity of the gaussian approximation for multi-user interference in ultra wide band impulse radio: from an inconvenience to an advantage. IEEE Trans Wireless Commun 8(11):5483–5489
9. Panaitopol D (2011) Ultra wide band ad-hoc sensor networks: a multi-layer analysis. PhD Thesis. Supélec and National University of Singapore
10. Mehbodniya A, Aissa S, Adachi F (2011) BER Analysis of DS-UWB system employing a laplace distribution model. IEICE Elect Expr 8(13):1089–1095
11. Ahmed QZ, Park KH, Alouini M-S (2015) Ultrawide bandwidth receiver based on a multivariate generalized gaussian distribution. IEEE Trans Wireless Commun 14(4):1800–1810
12. Deleuze AL, Ciblat P, Le Martret CJ (2005) Inter-symbol / inter-frame interference in time-hopping ultra wideband impulse radio system. In: IEEE International Conference on Ultra-Wideband. IEEE Press, p 6
13. Yoon E, Kim SY, Yun U (2015) A Time-Reversal-Based transmission using predistortion for intersymbol interference alignment. IEEE Trans Commun 63(2):455–465
14. Di Benedetto MG, Giancola G (2004) Understanding ultra wide band radio fundamentals, Prentice Hall
15. Chen Y et al. (2014) Time-Reversal Wireless paradigm for green internet of things: an overview. IEEE Internet Things J 1(1):81–98
16. Viteri-Mera CA, Teixeira FL, Sainath K (2015) Interference-nulling time-reversal beamforming for mm-Wave massive MIMO systems. In: IEEE International Conference on Microwaves, Communications, Antennas and Electronic Systems. IEEE Press, pp 1–5
17. Ma H, Wang B, Chen Y, Ray Liu KJ (2016) Time-Reversal Tunneling effects for cloud radio access network. IEEE Trans Wireless Commun 15(4):3030–3043
18. Palomar DP, Jiang Y (2006) MIMO transceiver design via majorization theory. Foundations and trends in communications and information theory 3(4)

19. Win MZ, Scholtz RA (1998) On the energy capture of ultra-wide bandwidth signals in dense multipath environments. *IEEE Commun Lett* 2(9):245–247
20. Cassioli D, Win MZ, Vatalaro F, Molisch AF (2002) Performance of Low-Complexity rake reception in a realistic UWB channel. In: *IEEE International Conference on Communications*, vol 2. IEEE Press, pp 763–767
21. Foerster JR, Pendergrass M, Molisch AF (2003) A channel model for ultrawideband indoor communication. In: *IEEE International Symposium on Wireless Personal Multimedia Communication*. IEEE Press
22. Ihara S (1978) On the capacity of channels with additive non-gaussian noise. *Elsevier Information and Control* 37(1): 34–39